Conference on Modelling Fluid Flow (CMFF'22)
The 18th International Conference on Fluid Flow Technologies
Budapest, Hungary, August 30 -September 2, 2022

CALCULATING PARTICLE RESIDENCE TIMES IN VESSEL GEOMETRIES WITH ANEURYSM

Dániel GYÜRKI[1], István SZIKORA[2], György PAÁL[3]

[1] Corresponding Author. Department of Hydrodynamic Systems, Faculty of Mechanical Engineering, Budapest University of Technology and Economics. Műegyetem rkp. 3, H-1111 Budapest, Hungary. Tel.: +36 1 463 1680, E-mail: dgyurki@hds.bme.hu
[2] Department of Neurointerventions, National Institute of Clinical Neurosciences, E-mail: h13424szi@ella.hu
[3] Department of Hydrodynamic Systems, Faculty of Mechanical Engineering, Budapest University of Technology and Economics. E-mail: paal@hds.bme.hu

ABSTRACT

Numerous studies focus on the formation and rupture of intracranial aneurysms which are saccular deformation of blood vessel walls on the brain arteries. Computational fluid dynamics (CFD) is often used in these studies. Our research concentrates on particle paths calculated from the results of CFD simulations of such malformations.

First, the flow field was obtained using lattice-Boltzmann simulations. A generalized inlet velocity signal was used, while at the outlets the flow rates were given. Paths of massless, passive particles were calculated, based on the flow field using a fourth order Runge-Kutta method. For each particle the reached outlet and the particle residence time (PRT) were recorded. The heart cycle was divided into 10 points evenly in time, and the particles were started at these time instances, hence obtaining 10 sets of outlets and PRTs for the particles.

The paths are strongly dependent on the flow velocity. Therefore, the instabilities, namely the fluctuating velocity arising during the decelerating phase strongly alter the paths of the particles through a stretching and folding action, resulting in filamentary fractal-like patterns. Our results show in the case of four geometries that the starting time of the particles during the heart cycle plays an important role.

Keywords: aneurysm, particle path, residence time

NOMENCLATURE

$\underline{r}$	$[m]$	position vector of particle
$\underline{v}$	$[m/s]$	velocity vector
t	$[s]$	time

Subscripts and Superscripts

0	at the start of the integration

1. INTRODUCTION

The main roles of blood vessels are to deliver nutrient- and oxygen-rich blood to the organs, and transfer the deoxygenated blood from the tissues back to the heart. The arterial system, which stems at the heart, is subjected to high blood pressures, therefore the arterial walls are prone to different malformations.

The two main malformations are stenosis and aneurysm. In case of the former, the lumen of the artery is narrowed down because of plaque formation in the inner wall of the vessels. The latter is the local dilatation of the arterial wall. Intracranial aneurysms (IA) are saccular, berry-like malformations on the wall of brain arteries, mainly found on the Circle of Willis.

IAs are usually asymptomatic but they carry a huge risk on the patient. If an aneurysm ruptures, it causes subarachnoid hemorrhage (SAH), which can result in the patient remaining dependent (~33%) or even cause death in half of the cases [1].

Different methods are available to prevent rupture when an aneurysm is found. Clipping the sac of the aneurysm is the oldest technique, the drawback is that this is an open skull surgery and not all aneurysms can be treated this way. During coiling, the sac is filled with a thin wire, therefore the blood coagulates there. The latest method is the use of braided devices called flow diverters (FD) which act as a hydrodynamic resistance between the parent vessel and the sac, and help the coagulation of the blood [2].

Because of the importance of the disease and the high number of affected people, much research concentrate on either the forming or the rupture of IAs, since these are unanswered questions to this day. Computational fluid dynamics (CFD) is a widely used tool of the studies in investigating the blood flow in vessel wall malformations.

Hemodynamic quantities derived from these simulations are correlated with the initiation location or the ruptured state of aneurysms [3]. However, numerous other parameters are used beside the hemodynamic factors, for example there are researchers who concentrate on simulating particle paths or concentrations in the geometries.

Reza et al. [4] computed and correlated six widely used residence time measures, stating that the appropriate one should be chosen according to the application. Rayz et al. [5] investigated Eulerian advection in IAs modelling the thrombus deposition, while Meschi et al. [6] even calculated drug delivery patterns in diseased arteries. Leemans et al. [7] compared particle residence times (PRT) of Lagrangian particles with aneurysm morphology and the ruptured state, and found that morphology plays an important role on PRT, while the correlation with the ruptured state is not significant.

In most cases, the flow through the arteries of the brain is considered laminar in CFD studies, since the Reynolds number does not exceed the 1000 region. However, some researchers found, that instabilities may arise during some parts of the cardiac cycle. For example, Valen-Sendstad et al. [8] express that in detailed CFD simulations, high frequency instabilities occurred in the carotid siphon right after the systolic peak, during the deceleration of the flow. Khan et al. [9] found a similar phenomenon in the simulation of flows in aneurysm geometries.

Závodszky et al. [10] showed that particles placed inside the flow of an aneurysm display a chaotic nature as fractal-like patterns emerged of the particles. Similar phenomenon was observed in the carotid bifurcation in 2D by Silva et al. [11]. However, as it was discussed earlier, flows in vessel wall malformations may initiate a transitional flow during the decelerating phase. Instabilities, which are considered as oscillations of the velocity, may have an enormous effect on PRT. Suh et al. [12] taken this effect into account during an abdominal aneurysm simulation by dividing the heart cycle to 10 points and calculated a mean PRT by averaging the PRTs of particles released at each point. This takes into account the release time, but does not show the effect of the decelerating phase of the heart cycle.

During our research, we investigated the particle paths with different particle release time points to qualitatively show the effect of the flow instabilities arising from the deceleration of the flow.

2. METHODS

2.1. Geometry preparation

The first step of the study is to obtain real aneurysm geometries and prepare them for the simulation.

Our medical partner provides digital subtraction angiography (DSA) images of patients with IAs found on one or more of their brain arteries. The resolution of the images was 0.22 mm. The DSA images are segmented using 3DSlicer [13], then additional smoothing was applied using MeshLab (version 1.3.2) [14]. The 3D geometries were evaluated based on our previous experience and consultations with neurointerventionalists.

Following the segmentation and smoothing, openings of the geometries are extended in order to limit the effects of the imposed boundary conditions. Last, the geometry was box-cut in a way that the inlet plane is parallel with the XY plane of the box. These procedures were made with an in-house script written in Python.

2.2. Flow simulation

Lattice-Boltzmann method (LBM) was used during the flow simulations. This method originates in the lattice gas automaton, and is used to solve numerically a fluid flow problem. But unlike the commercial methods, which usually solve the discretised Navier-Stokes equations, like the finite volume method, LBM calculates the collision and streaming of fictive particles. Macroscopic quantities, like pressure or velocity can be calculated based on the probability density function of these particles. This way the Navier-Stokes equations are solved on a mesoscopic scale. One of the greatest advantage of the LBM is its potential of parallelisation, therefore the application of high performance computers is possible, which means that the computational time can be reduced greatly compared to regular fluid flow simulations.

The LBM requires a rectangular domain discretised into a uniform grid, hence the box cut mentioned in the previous subsection. The preparation of the grid is named voxelisation, and was performed using an in-house Python script.

During voxelisation, each voxel is assigned either the Unused or the Fluid value. Unused voxels are outside the geometry and no equation is calculated in them. The fluid domain is formed from Fluid voxels, that is where the equations of the flow simulation are calculated. The Fluid voxels can be further assigned as boundary conditions, like wall, inlet or outlets.

The only parameter of the voxel domain is the voxel size. Too large voxel size results in inaccurate results, while too small voxel size increases computational cost unreasonably. In our study, the voxel size was around 0.06 *mm* in each case, resulting in around 5 million Fluid voxels.

At the inlet boundary, parabolic velocity profile was prescribed. The maximum of the parabola is controlled throughout the time by a 1 *s* long generic signal from the literature. This signal can be seen in Figure 1. The Reynolds number at the inlet is set to be 250, calculated from the average of the parabola at the maximum value of the signal and the diameter of the inlet vessel.

The outlet with the smallest area is defined as a pressure outlet in order to avoid overdefining the simulation. The other outlets are set as velocity outlets with parabolic velocity profiles. Their velocities are calculated based on the Murray's law [15], which splits the volumetric flow rate based on the areas of the outlets. Bounce back scheme is prescribed at the wall of the fluid geometry.

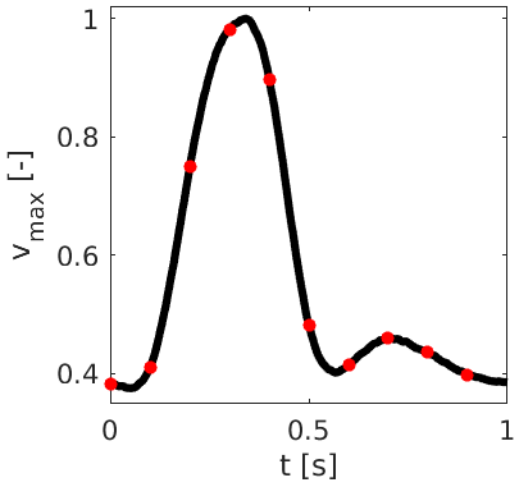

Figure 1. Signal controlling the velocity of the inlet

The time step of the simulation is determined according to a stability criterion of the LBM. At each simulation it was around 1.5×10^{-5} *s*, while the velocity field was saved at every 0.01 *s*, resulting in 100 flow fields. The simulations were made using an in-house code based on Palabos [16].

2.3. Particle tracing

After obtaining the flow field through the time, the last step is to acquire the paths of particles. The particles are considered as massless and passive, therefore they instantaneously pick up the velocity of a given point in the flow field (see Eq. (1)), and do not have an effect on the flow itself. To acquire the position of such particles at a given time, one has to integrate the velocity field in time, from a given initial position and time, see Eq. (2).

$$\dot{\underline{r}}(t) = \frac{d\underline{r}(t)}{dt} = \underline{v}\big(\underline{r}(t), t\big) \tag{1}$$

$$\underline{r}(t) = \int_{t_0}^{t} \underline{v}\big(\underline{r}(t'), t'\big)\, dt' + \underline{r}(t_0) \tag{2}$$

The paths are calculated using a fourth order Runge-Kutta method written in C++. The time step of the integration is set to 10^{-4} *s*. Choosing too small integration step may result in an unreasonably slow computation, while too large integration step could be inaccurate. The integration is done until 10 heart cycles in order to let enough time for the particles to leave the domain. The PRT (the time for the particle to leave the domain) and the outlets are recorded for every particle.

The paths of 1 million particles are calculated for every case. These particles are started from a plane near the inlet. For each aneurysm geometry, 10 different integrations were made, starting from different time instances. The length of the heart cycle was divided into 10 points, which are marked with red dots in Fig. 1. These 10 time points are the starting times of the path calculation resulting in a qualitative temporal investigation.

Four intracranial aneurysm geometries were investigated in this study. The procedure described previously was carried out for each geometry, the results for one geometry are 10 set of PRT and outlet for the 1 million particles.

Contour plots were made in order to investigate the effect of the release time of the particles. The points of the starting plane are coloured according to the outlet number of the particle started from that given point.

3. RESULTS

Figure 2 shows the results for the first case. The geometry can be seen at the top of the figure. The red plane at the bottom of the geometry is the starting plane of the particles. The aneurysm sac is coloured blue, and the outlets are coloured differently. Fig. 2 also contains the starting points coloured according to the outlet colour of the geometry for the 10 different starting times ordered in a 5 by 2 grid.

As it is seen, there are remarkable differences between the contour plots. Usually, it takes the particles 0.5-0.7 seconds to leave the domain in this smaller geometry. Therefore, if the particles are released at the start of the heart cycle, most of them have already left the aneurysm, or even the domain when the systolic peak (maximum velocity) takes place. That is the reason why there are simple, well-defined regions on that subfigure. However, if the particles are released later in the heart cycle, more of them are yet to reach the aneurysm at the systolic peak and when the decelerating phase starts. As a result of this, the subfigures corresponding to the 0.3 and 0.4 *s* starting time show complex, filamentary structures, similarly to Závodszky et al. [10].

This great dependence on the initial position and the resulting filamentary structure are signs of chaotic advection of the particles. There is a strong connection between the instabilities arising at the decelerating phase of the heart cycle and the chaotic nature of the particle paths, as Eq. (2) suggests.

The signal used in this study (Fig. 1) varies less after the decelerating phase, therefore the structures appearing in the subsequent subfigures are less complicated, and similar to each other. Therefore, one can assume, that the flow stabilises after the deceleration phase.

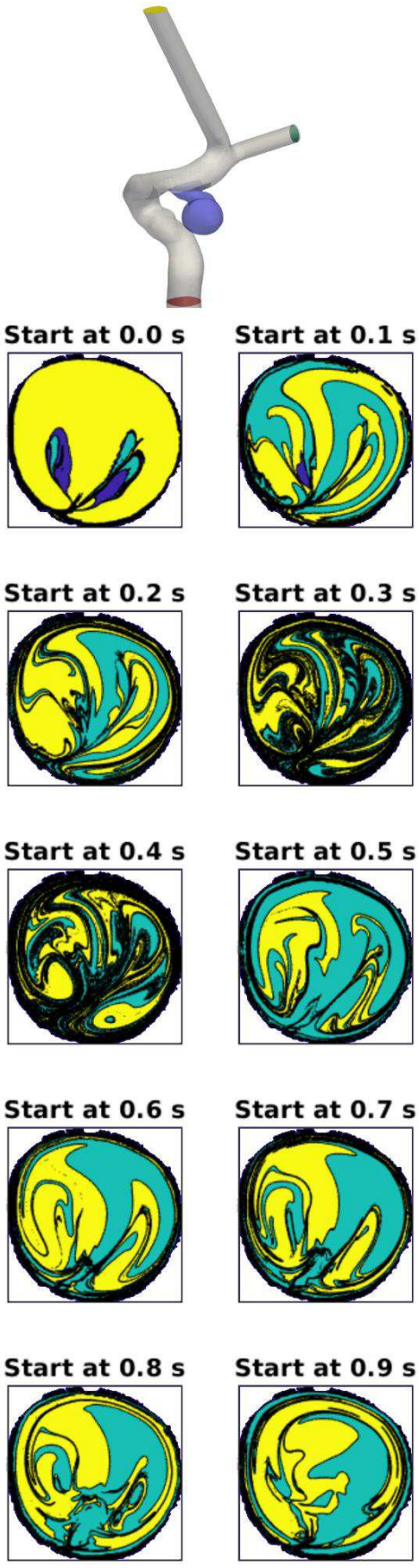

Figure 2. The geometry and the inlet coloured according to the outlets for the first aneurysm

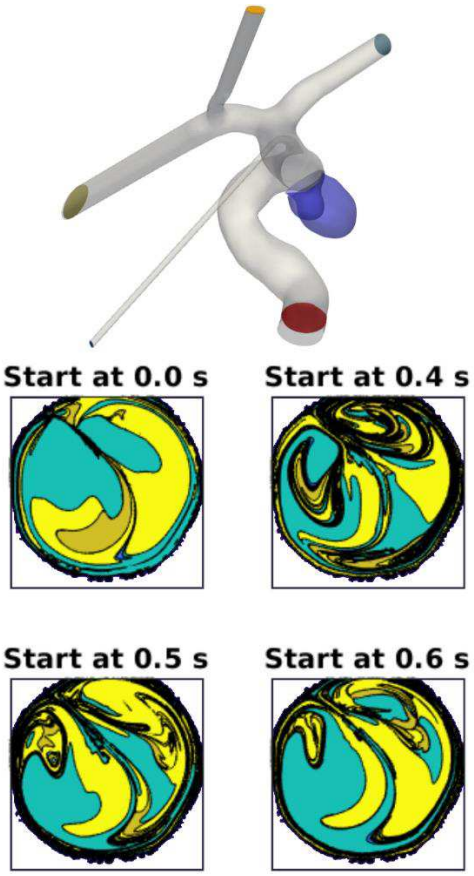

Figure 3. The geometry and the inlet coloured according to the outlets for the second aneurysm

Only four starting times are shown for the rest of the aneurysm geometries in order to concentrate on the greatest differences. Figure 3 shows the results for the second geometry. This geometry has 4 outlets and slightly more bends, and generally it takes a little longer time for the particles to reach the aneurysm, or leave the domain. Therefore, the 0.4, 0.5 and 0.6 *s* cases are shown, beside the 0.0 *s* case. The red plane at the bottom is the plane of the starting points, and the subfigures are coloured according to the colours on the geometry.

Similarly to the previous geometry, the particles released at the start of the heart cycle show a simple structure, only few folded patterns appear, the different regions are well-defined. In contrast with this, the other subfigures display the complex filamentary structures, mainly at the top part of the starting plane. Presumably, the slight bends stabilise the flow, therefore the magnitude of the instabilities may be limited, affecting the paths of the particles less. It was also found by checking the paths, that the filamentary part of the inlet is the place, from where the particle paths travel close to the aneurysm sac, which swirls the flow field, hence the complexity of the patterns.

The results of other starting times, which are not shown in the figure, are similar to the first aneurysm, they show less folded, filamentary structure.

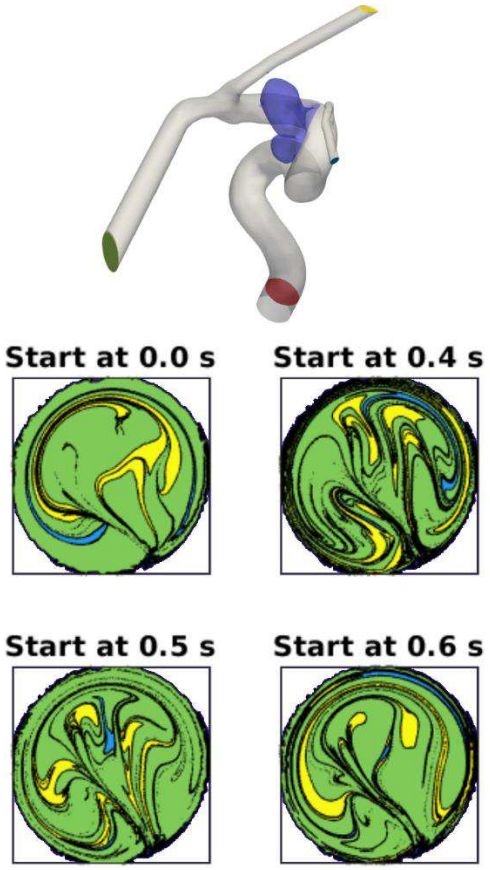

Figure 4. The geometry and the inlet coloured according to the outlets for the third aneurysm

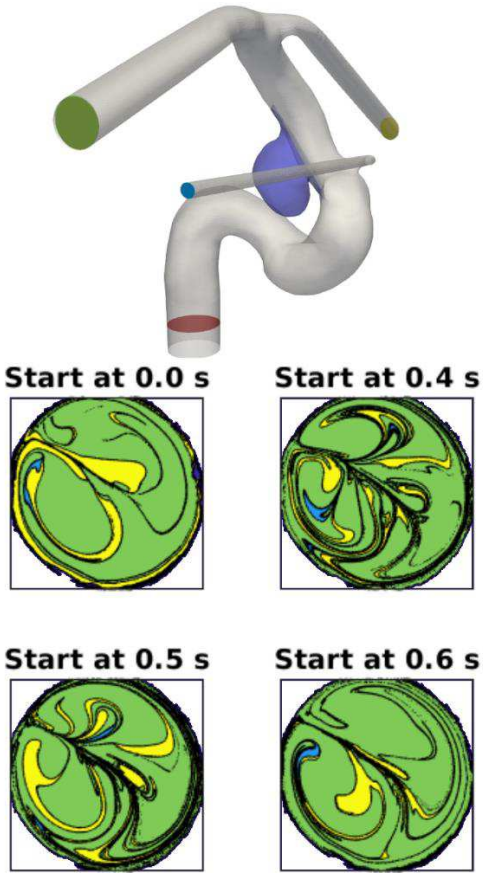

Figure 5. The geometry and the inlet coloured according to the outlets for the fourth aneurysm

The results of the third aneurysm can be seen in Figure 4. Again, only the most different three starting time instances are shown, beside the start of the cycle. This geometry has three outlets and is the most bendy of the four. The bending may be the reason why the results of the case started at the beginning of the heart cycle show little filamentary structure. The secondary flows originating from the bends fold the paths of the particles already. However, it is clearly shown in the subfigures of Fig. 4, that the particles released in the decelerating phase of the heart cycle display a more complex structure, similarly to the previous cases.

They are not shown in Fig. 4, but the results of the last three points of the heart cycle are almost identical, the small deceleration after diastolic peak of the inlet curve creates so small scale instabilities, or none at all, that the paths are not affected by them.

Figure 5 shows the last aneurysm geometry and part of the results. Similar conclusions can be drawn based on this figure to the previous cases. The first subfigure displays a slight folded structure, for example because of the bends or the wide neck of the aneurysm. The rest of the subfigures show the previously mentioned complex structures. Similarly to the third case, the not shown results of the last three points are almost the same. The instabilities arising in this flow may be limited.

Altogether, all four results are similar. The instabilities during the deceleration phase of the heart cycle have an enormous effect on the particle paths, resulting in a folded, fractal-like structure. After the deceleration, the flow is stabilised and so are the paths, as indicated by the less complex structures. The increase of the complexity and foldedness of the displayed structure should be quantified and correlated with morphological factors.

4. CONCLUSIONS

This study focused on following particle paths inside intracranial aneurysms. These particles can model the real particles or molecules, which can be the part of physiological processes, like blood coagulation or drug adsorption. However, as the paths depend greatly on the local velocity, the arising instabilities of a decelerating flow alter them greatly.

Transient lattice-Boltzmann simulations were performed to obtain the flow field in case of four patient-specific 3D IA geometries. Based on the velocity fields, the paths of 1 million particles started near from the inlet are calculated. The heart cycle was divided to 10 points, and the path calculation was repeated starting at each point. Particle residence times and reached outlets were recorded.

All of the four geometries display similar tendency, particles released closer to the decelerating

phase show more complex, fractal-like structure based on the reached outlet. This is the result of the stretching and folding action of the arising instabilities. These results show, that the release time instance should be taken into consideration during particle tracing in pulsatile flows.

ACKNOWLEDGEMENTS

This research was supported by the National Brain Research Program under the Contract Number 2017-1.2.1-NAP-2017-00002, and by the National Research, Development, and Innovation Fund of Hungary under Grant TKP2021-EGA-02. The conference participation was supported by the Végh Gábor Neurointervention Fundation.

REFERENCES

[1] van Gijn, J, and Rinkel, G.J., 2001, ”Subarachnoid haemorrhage: diagnosis, causes and management”, *Brain*, Vol. 124(2), pp. 249-278.

[2] Fiorella, D., Lylyk, P., Szikora, I., Kelly, M.E., Albuquerque, F.C., McDougall, C.G., and Nelson, P.K., 2008, ”Curative cerebrovascular reconstruction with the pipeline embolization device: the emergence of definitive endovascular therapy for intracranial aneurysms”, *J Neurointerv Surg*, Vol. 1(1), pp. 56-65.

[3] Qian, Y., Takao, H., Umezu, M., and Murayama, Y., 2011, ”Risk Analysis of Unruptured Aneurysms Using Computational Fluid Dynamics Technology: Preliminary Results”, *AJNR Am J Neuroradiol*, Vol. 32(10), pp. 1948-1955.

[4] Reza, M.M.S., and Arzani, A., 2019, ”A critical comparison of different residence time measures in aneurysms”, *J Biomech*, Vol. 88, pp. 122-129.

[5] Rayz, V.L., Boussel, L., Ge, L., Leach, J.R., Martin, A.J., Lawton, M.T., McCulloch, C., and Saloner, D., 2010, ”Flow residence time and regions of intraluminal thrombus deposition in intracranial anuerysms”, *Ann Biomed Eng*, Vol. 38(10), pp. 3058-3069.

[6] Meschi, S.S., Farghadan, A., and Arzani, A., 2021, ”Flow topology and targeted drug delivery in cardiovascular disease”, *J Biomech*, Vol 119, pp. 110307.

[7] Leemans, E.L., Cornelissen, B.M.W., Rosalini, G., Verbaan, D., Schneiders, J.J., van den Berg, J.J., Vandertop, W.P., van Bavel, E.T., Slump, C.H., Majoie, C.B.L.M., and Marquering, H.A., 2019, ”Impact of Intracranial Aneurysm Morphology and Rupture Status on the Particle Residence Time”, *J Neuroimaging*, Vol. 29(4), pp. 487-492.

[8] Valen-Sendstad, K., Piccinelli, M., and Steinman, D.A., 2014, ”High-resolution computational fluid dynamics detects flow instabilities in the carotid siphon: Implications for aneurysm initiation and rupture?”, *J Biomech*, Vol. 47(12), pp. 3210-3216.

[9] Khan, M.O., Chnafa, C., Gallo, D., Molinari, F., Morbiducci, U., Steinman, D.A., and Valen-Sendstad, K., 2017, ”On the quantification and visualization of transient periodic instabilities in pulsatile flows”, *J Biomech*, Vol. 52, pp. 179-182.

[10] Závodszky, G., Károlyi, G., and Paál, G., 2017, ”Emerging fractal patterns in a real 3D cerebral aneurysm”, *J Theor Biol*, Vol. 368, pp. 95-101.

[11] Silva, I.M., Schelin, A.B., Viana, R.L., and Caldas, I. L., 2020, ”Transport of blood particles: Chaotic advection even in a healthy scenario”, *Chaos*, Vol. 30(9), pp. 093135.

[12] Suh, G., Les, A.S., Tenforde, A.S., Shadden, S.C., Spilker, R.L., Yeung, J.J., Cheng, C.P., Herfkens, R.J., Dalman, R.L., and Taylor, C.A., 2011, ”Quantification of Particle Residence Time in Abdominal Aortic Aneurysms Using Magnetic Resonance Imaging and Computational Fluid Dynamics”, *Ann Biomed Eng*, Vol. 39(2), pp. 864-883.

[13] Fedorov, A., Beichel, R., Kalpathy-Cramer, J., Finet, J., Fillion-Robin, J.C., Pujol, S., Bauer, C., Jennings, D., Fennessy, F.M., Sonka, M., Buatti, J., Aylward, S.R., Miller, J.V., Pieper, S., and Kikinis, R., 2012, ”3D Slicer as an Image Computing Platform for the Quantitative Imaging Network”, *Magn Reson Imaging*, Vol. 30(9), pp. 1323-1341.

[14] Cignoni, P., Callieri, M., Corsini, M., Dellepiane, M., Ganovelli, F., Ranzuglia, G., 2008, ”MeshLab: an Open-Source Mesh Processing Tool”, *Sixth Eurographics Italian Chapter Conference*, Salerno, Italy, pp. 129-136.

[15] Chnafa, C., Brina, O., Pereira, V.M., and Steinman, D.A., 2018, ”Better Than Nothing: A Rational Approach for Minimizing the Impact of Outflow Strategy on Cerebrovascular Simulations.”, *AJNR Am J Neuroradiol*, Vol. 39(2), pp. 337-343.

[16] Latt, J., Malaspinas, O., Kontaxakis, D., Parmigiani, A., Lagrava, D., Brogi, F., Belgacem, M.B., Thorimbert, Y., Leclaire, S., Li, S., Marson, F., Lemus, J., Kotsalos, C., Conradin, R., Coreixas, C., Petkantchin, R., Raynaud, F., Beny, J., and Chopard, B., 2021, ”Palabos: Parallel Lattice Boltzmann Solver”, *Comput Math,* Vol. 81, pp. 334-350.